NASA/TM—20250006213

Hover Validation and Acoustic Baseline (HVAB) Rotor Blade C81 Table Generation

Dr. Jason K. Cornelius
Ames Research Center, Moffett Field, California

June 2025

NASA STI Program ... in Profile

Since its founding, NASA has been dedicated to the advancement of aeronautics and space science. The NASA scientific and technical information (STI) program plays a key part in helping NASA maintain this important role.

The NASA STI program operates under the auspices of the Agency Chief Information Officer. It collects, organizes, provides for archiving, and disseminates NASA's STI. The NASA STI program provides access to the NTRS Registered and its public interface, the NASA Technical Reports Server, thus providing one of the largest collections of aeronautical and space science STI in the world. Results are published in both non-NASA channels and by NASA in the NASA STI Report Series, which includes the following report types:

- TECHNICAL PUBLICATION. Reports of completed research or a major significant phase of research that present the results of NASA Programs and include extensive data or theoretical analysis. Includes compilations of significant scientific and technical data and information deemed to be of continuing reference value. NASA counter-part of peer-reviewed formal professional papers but has less stringent limitations on manuscript length and extent of graphic presentations.

- TECHNICAL MEMORANDUM. Scientific and technical findings that are preliminary or of specialized interest, e.g., quick release reports, working papers, and bibliographies that contain minimal annotation. Does not contain extensive analysis.

- CONTRACTOR REPORT. Scientific and technical findings by NASA-sponsored contractors and grantees.

- CONFERENCE PUBLICATION. Collected papers from scientific and technical conferences, symposia, seminars, or other meetings sponsored or co-sponsored by NASA.

- SPECIAL PUBLICATION. Scientific, technical, or historical information from NASA programs, projects, and missions, often concerned with subjects having substantial public interest.

- TECHNICAL TRANSLATION. English-language translations of foreign scientific and technical material pertinent to NASA's mission.

Specialized services also include organizing and publishing research results, distributing specialized research announcements and feeds, providing information desk and personal search support, and enabling data exchange services.

For more information about the NASA STI program, see the following:

- Access the NASA STI program home page at http://www.sti.nasa.gov

- E-mail your question to help@sti.nasa.gov

- Phone the NASA STI Information Desk at 757-864-9658

- Write to:
  NASA STI Information Desk
  Mail Stop 148
  NASA Langley Research Center
  Hampton, VA 23681-2199

NASA/TM—20250006213

Hover Validation and Acoustic Baseline (HVAB) Rotor Blade C81 Table Generation

Dr. Jason K. Cornelius
Ames Research Center, Moffett Field, California

National Aeronautics and
Space Administration

Ames Research Center
Moffett Field, CA 94035-1000

June 2025

ACKNOWLEDGMENTS

I would like to thank Stephen Wright, Wayne Johnson, Christopher Silva, Thomas Norman, and Sesi Kottapalli for their contributions to this work. Many thanks also to Ethan Romander and Kristen Kallstrom for their support in setting up and running AFTGen on the NASA High-End Compute Capability. Along those lines, I want to thank the NASA Advanced Supercomputing Division for their assistance in using the NASA High-End Computing Capability computational resources. Lastly, many thanks to William Warmbrodt and Carl Russell for their support of this work. This work was supported by the NASA Revolutionary Vertical Lift Technology Project.

This report is available in electronic form at

http://ntrs.nasa.gov

Contents

List of Figures

List of Tables

Nomenclature

ARC	Ames Research Center
BET	Blade Element Theory
CA	Comprehensive Analysis
CFD	Computational Fluid Dynamics
CPU	Central Processing Unit
GCS	Grid Convergence Study
GUI	Graphical User Interface
HECC	High-End Computing Capability
HVAB	Hover Validation and Acoustic Baseline
NACA	National Advisory Committee for Aeronautics
NASA-HECC	NASA High-End Computing Capability
NFAC	National Full-Scale Aerodynamics Complex
PSP	Pressure Sensitive Paint

Hover Validation and Acoustic Baseline (HVAB) Rotor Blade C81 Table Generation

Dr. Jason K. Cornelius

Ames Research Center
Moffett Field, California

Abstract

The Hover Validation and Acoustic Baseline (HVAB) blade set has been jointly developed by the U.S. Army Combat Capabilities Development Command Aviation & Missile Center (CCDC AvMC) and the NASA Revolutionary Vertical Lift Technology (RVLT) Project. The 4-bladed HVAB rotor was tested in the NASA Ames Research Center's (ARC) National Full-Scale Aerodynamics Complex (NFAC) 80- by 120-Foot Wind Tunnel. This document summarizes the creation of C81 airfoil performance lookup tables based on the conditions tested during the 2022 NFAC entry. The tables were generated with approximately 1,500 OVERFLOW CFD calculations run on the NASA High-End Computing Capability (HECC). The simulations were run fully turbulent using a Spalart-Allmaras turbulence closure and are 2nd order accurate in time and 4th order accurate in space. The methods used for both the simulation setup and C81 table creation, including blending the OVERFLOW data into experimental data post-stall, are detailed throughout this work. The C81 tables are embedded in Appendix I of this document for public distribution.

1 Background Information

The Hover Validation and Acoustic Baseline (HVAB) test program was conducted at NASA Ames Research Center (ARC) in 2022, Ref. [1]. The experimental test campaign took place inside the National Full-Scale Aerodynamics Complex (NFAC) 80- by 120-Foot Wind Tunnel test section as shown in Figure 1. The program conducted a "model-scale hover test of a 4-bladed, 11.08-ft diameter rotor representative of a 'modern' multi-bladed helicopter." The primary objective of this experimental test campaign was to create a validation data set for state-of-the-art analysis tools. Measurements included rotor performance, blade airloads, boundary layer transition locations, blade deflections, and wake geometry. This data is available on the NASA ARC Aeromechanics Office website, Ref. [2]. This work presents the methodology used to create airfoil performance look-up tables for the HVAB rotor airfoils under representative conditions from the test.

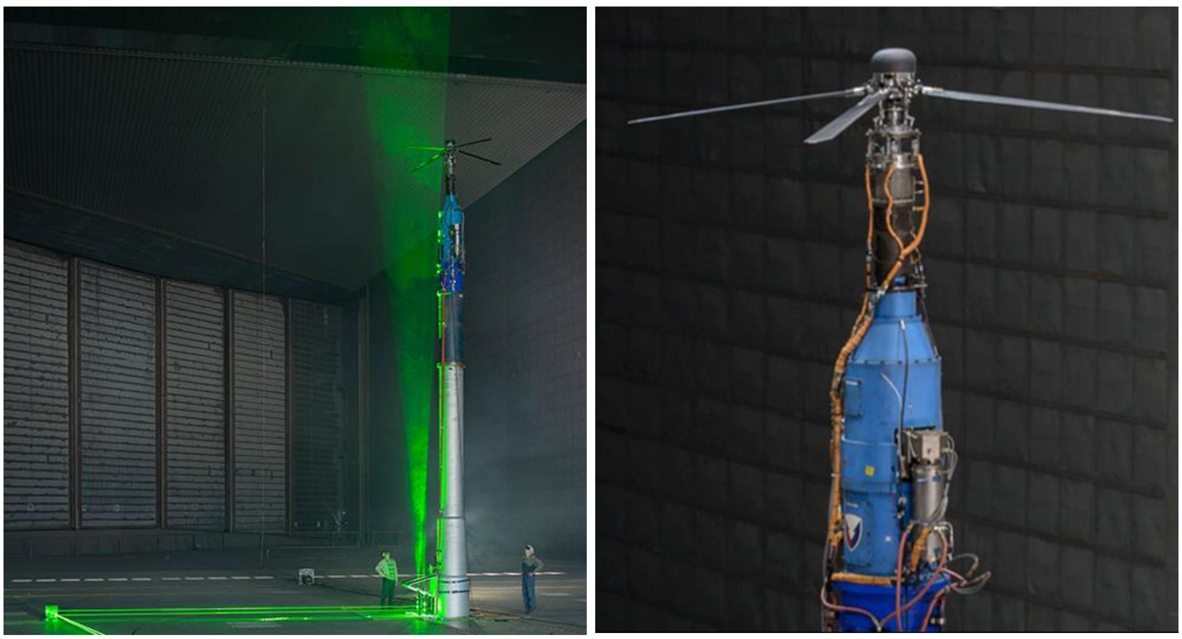

Figure 1. HVAB Rotor Test in the NASA Ames Research Center NFAC 80- by 120-Foot Wind Tunnel.

1.1 Airfoil Performance Look-up Tables: C81 Tables

In the aerospace community, airfoil look-up tables are often used in low- and mid-fidelity tools for the prediction of aircraft and rotorcraft performance. In the rotorcraft community, these airfoil performance look-up tables are commonly formatted as C81 tables that report airfoil performance as a function of both angle-of-attack and local Mach number. The naming convention (i.e., C81) is one of historical context dating back to the early days of rotorcraft comprehensive analysis programs on digital computers. Since that time, these airfoil performance look-up tables for use in rotorcraft applications are referred to simply as "C81 tables."

Methods such as Blade Element Theory (BET), Comprehensive Analysis (CA), and even some hybrid Computational Fluid Dynamics (CFD)-BET approaches use C81 tables to yield fast yet meaningful results. Obtaining accurate results requires each rotor design to have a tailored set of C81 tables with the given airfoils at appropriate Reynolds and Mach numbers. An example rotor blade airfoil table discretization is shown in Figure 2. The rotor blade is discretized into 10 stations to capture radial changes in airfoil chord, thickness, and camber. Higher discretization is important for modeling rotors with large radial variations in chord as well as variable-speed rotor systems. These systems have both the rotor blade geometry and aerodynamic conditions changing as a function of radial position and rotor speed. Past studies by Patt and

Youngren, Ref. [3], and Cornelius and Schmitz, Ref. [4], document both the need for a finer discretization of airfoil look-up tables and the improvements obtained through their implementation.

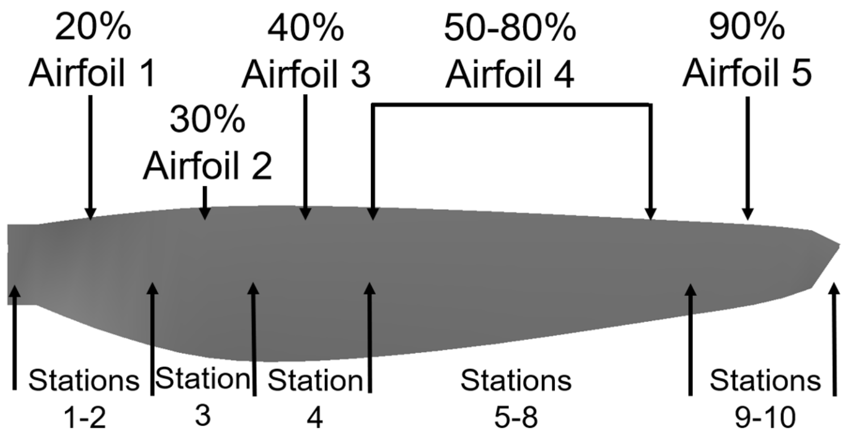

Figure 2. Airfoil Look-up Table Discretization for Variable-Speed Rotors with Large Chord Changes.

State-of-the-art approaches for airfoil look-up table generation involve two-dimensional airfoil CFD analyses such as OVERFLOW or ARC2D, Refs. [5-6]. These tables are sometimes created with existing experimental data but are then limited to the Mach and Reynolds numbers tested. Many experimental datasets are also proprietary and thus not publicly accessible. Other times they are generated using lower-fidelity computational tools. This work presents new C81 tables that were developed using OVERFLOW for the HVAB rotor.

1.2 Summary of HVAB Rotor

The HVAB rotor was defined in NASA/TM-2020-5002153, "Hover Validation and Acoustic Baseline Blade Set Definition," Ref. [7]. This NASA Technical Memorandum provides detailed information on the HVAB rotor blade, including the outer mold line, the structural properties, and the instrumentation included on the rotor for testing. Tables 1-2 and Figure 3 are reproduced below from that work.

Table 1. HVAB Rotor Blade Characteristics (Reproduced).

Number of Blades, N_b	4
Blade Radius, R (in)	66.50
Blade Chord, c (in)	5.45
Rotor Geometric Solidity, σ	0.1033
Rotor Airfoil	RC series
Blade Twist Distribution	Linear
Blade Twist (deg)	-14

Table 2. HVAB Rotor Blade Planform (Reproduced).

r/R	Twist	c	Sweep	0.25c Position ΔX	ΔY	ΔZ	Airfoil
-	(deg)	(in)	(deg)	(in)	(in)	(in)	-
0.13985	8.20	5.45	0	9.300	0	0	$RC(4)-12$
0.16722	8.20	5.45	0	11.120	0	0	$RC(4)-12$
0.25188	7.01	5.45	0	16.750	0	0	$RC(4)-12$
0.65128	1.40	5.45	0	43.310	0	0	$RC(4)-12$
0.70120	0.70	5.45	0	46.630	0	0	$RC(4)-10$
0.80075	-0.70	5.45	0	53.250	0	0	$RC(4)-10$
0.85053	-1.40	5.45	0	56.560	0	0	$RC(6)-08$
0.95023	-2.80	5.45	0	63.190	0	0	$RC(6)-08$
1.00000	-3.50	3.27	30	66.500	-1.911	0	$RC(6)-08_T$

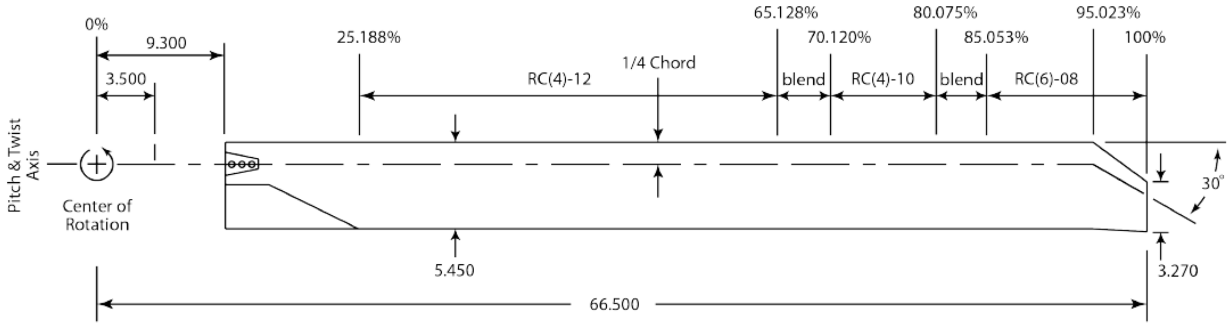

Figure 3. HVAB Planform (Reproduced).

2 HVAB C81 Table Generation

This section details the process used to create the C81 airfoil performance lookup tables for the HVAB rotor. The rotor blade geometry and discretization are first discussed. This is then followed by the operating conditions of interest relevant to both the experimental testing and prior computational analyses. Airfoil simulation setup using the OVERFLOW solver in a wrapper called “AFTGen” is then described along with a brief discussion of the mass-parallelization of these simulations on the NASA High-End Computing Capability (NASA-HECC).

2.1 HVAB Rotor Blade Discretization

The HVAB rotor is fully defined by three RC-series airfoils as documented in Table 2 and Figure 3. They are the RC(4)-12, RC(4)-10, and the RC(6)-08. The rotor tip region (the outer most 5% rotor radius) has a slightly higher trailing edge thickness and is denoted as the RC(6)-08$_T$. Dense coordinate files and rotor planform definitions are included in Reference [7] and reproduced in Appendix I. A single C81 airfoil performance lookup table has been created for each of these four coordinate files. Additional details regarding these airfoil geometries and some available experimental data are found in References [8-11].

2.2 Flow Conditions

The average flow conditions from the NFAC experimental testing are reported in Table 3. These conditions are very close to standard sea-level atmospheric properties. In the spirit of generating generalized C81 airfoil performance lookup tables for the HVAB rotor, standard sea-level atmospheric properties were used in the OVERFLOW simulations to derive Reynolds number. The values used are reported in Table 4.

Table 3. Average Flow Conditions from NFAC Experimental Testing.

Aerodynamic Property	Value (imperial)	Value (metric)
Atmospheric Pressure	2122.00794 $\mathrm{lb/ft^2}$	101,602.18 Pa
Static Temperature	56.89403856 °F	286.98 K
Density	0.002383816 $\mathrm{slugs/ft^3}$	1.22857 $\mathrm{kg/m^3}$
Dynamic Viscosity	3.726*10^{-7} $\mathrm{lbf * s/ft^2}$	0.00001784 Pa $*$ s
Speed of Sound	1114.08 ft/s	339.571 m/s

Table 4. Standard Sea-Level Atmospheric Properties Used in OVERFLOW.

Aerodynamic Property	Value (imperial)	Value (metric)
Atmospheric Pressure	2116.2 $\mathrm{lb/ft^2}$	101,325.0 Pa
Static Temperature	59.0 °F	288.15 K
Density	0.002378 $\mathrm{slugs/ft^3}$	1.225 $\mathrm{kg/m^3}$
Dynamic Viscosity	3.737*10^{-7} $\mathrm{lbf * s/ft^2}$	0.00001789 Pa $*$ s
Speed of Sound	1125.33 ft/s	343.0 m/s

Experimental testing was conducted at the following blade-tip Mach numbers: $\mathrm{M_{tip}} = 0.6, 0.65, 0.675$, Ref. [2]. High-fidelity computational predictions for the HVAB rotor were also published ahead of the experimental testing for one additional blade-tip Mach number of 0.58, which was relevant to the previously tested Pressure Sensitive Paint (PSP) experimental campaign, Ref. [12]. The rotor geometry from Figure 3 was combined with the aerodynamic properties in Table 4 and the blade-tip Mach numbers in Table 5 to assess the chord-based Reynolds number along the blade for the various test conditions. Table 6 reports the average Reynolds number for each airfoil section, at various radial locations. These average values were used to inform the OVERFLOW grid convergence study (GCS), which is detailed in the next section.

Table 5. HVAB Rotor Simulated Blade-tip Mach Numbers.

Type of Data	Blade-tip Mach Number
Experimental	0.6, 0.65, 0.675
Computational	0.58, 0.6, 0.65, 0.675

Table 6. Average Reynolds Number Along the HVAB Blade at $M_{tip} = 0.626$.

Airfoil	Radial Locations	Average Reynolds Number
RC(4)-12	15-30%	450,738
RC(4)-12	30-48%	808,221
RC(4)-12	48-67.5%	1,181,245
RC(4)-10	67.5-82.5%	1,523,185
RC(6)-08	82.5-95%	1,818,496
RC(6)-08_T	95-100%	1,570,812

2.3 AFTGen Wrapper for OVERFLOW

The tool AFTGen was used in this work as a wrapper for OVERFLOW, Ref. [13]. AFTGen provides a user-friendly Graphical User Interface (GUI) that provides a means to import airfoil coordinate files, create grids, and adjust solver settings. Although it supports various numerical flow solvers, the CFD solver OVERFLOW was used in this work. AFTGen automates the process of running batches of these two-dimensional airfoil calculations by handling the automatic distribution, monitoring, and solution convergence for some user-defined number of simulations. The simulations in this work used Spalart-Allmaras turbulence closure and were 2nd order accurate in time and 4th order accurate in space. AFTGen also automates the solution process by starting with steady-state calculations and switching to an unsteady solution if the operating condition is beyond +/-10 degrees, or if the solution monitor detects an unsteady output.

Grid convergence studies (GCS) were carried out using the RC4-12 and RC6-08 airfoils (i.e., the thickest inboard section and a thinner outboard section). Figure 4 shows an example of the AFTGen generated grid for the RC4-12 airfoil along with a close-up of the blunt trailing edge. The study assessed grid point convergence at low and high Mach numbers of 0.3 and 0.7, respectively. The appropriate Reynolds number was calculated using the sea-level standard conditions and the HVAB rotor chord of 5.45 inches. These simulation conditions are reported in Table 7.

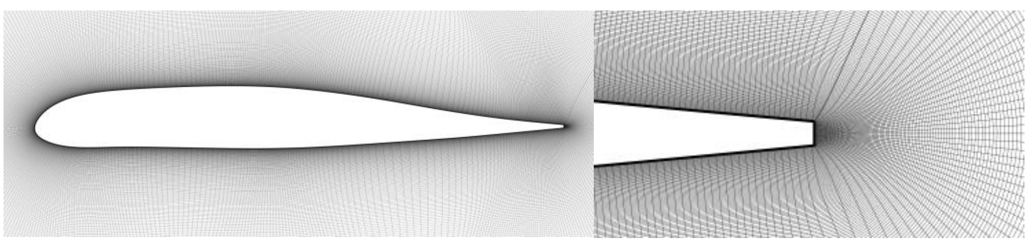

Figure 4. O-Grid for the RC4-12 Airfoil in AFTGen.

Table 7. Grid Convergence Study Simulation Conditions.

Mach Number	Reynolds Number
0.3	975,374
0.7	2,275,874

The GCS baseline grid (developed based on prior experience) consisted of 501 periodic cells, 601 normal cells, and 41 cells across the blunt trailing edge. The O-grid boundary was 200 chord lengths away and the y+ on the airfoil was set to one. OVERFLOW computations (results) using higher refinement grids (with 601 periodic cells, 701 normal cells, and 51 trailing edge cells) were within 1% of the baseline grid results for 97.2% of comparisons across lift, drag, and pitching moment coefficients for angles of attack of 0, 5, and 10 degrees. The two outliers (2/72 total comparisons) were within 2% of the baseline. Both outliers were the airfoil pitching moment coefficient at 5 degrees angle of attack and Mach number of 0.7. This GCS verified the baseline grid as adequate for the HVAB airfoil family.

2.4 Running on the NASA High-End Computing Capability

The AFTGen tool is typically used on a personal workstation, with the maximum number of simultaneous solver instances equal to the number of processors on the computer's Central Processing Unit (CPU). The Aeromechanics Office at NASA Ames Research Center has successfully run AFTGen on the NASA-HECC to access larger compute power. The tool can be run either through the GUI with X11 forwarding or can be run without the GUI and controlled with a Python or bash script as a wrapper for AFTGen. This work used the NASA-HECC Intel Broadwell and Skylake nodes with 28 cores and 40 cores, respectively.

To make generalized airfoil performance look-up tables that would also be effective for the HVAB rotor analyses, a wide range of Mach numbers was simulated over a wide range of angles of attack. The conditions simulated are reported in Table 8, and amount to 369 OVERFLOW calculations per airfoil, or 1,476 total simulations. These simulations were run using multiple nodes on the NASA-HECC.

Reynolds number was calculated using the HVAB chord of 5.45 inches for the RC4-12, RC4-10, and RC6-08. This yielded a chord-based Reynolds number at sonic conditions of 3,251,248. For the RC6-08$_T$, an average chord value was used to calculate Reynolds number. The chord-based Reynolds number for a sonic condition was 2,567,070.

Table 8. Simulation Conditions Run in OVERFLOW for Each HVAB Airfoil.

Metric	Simulation Conditions
Mach Number	0.1, 0.2, 0.3, 0.4, 0.5, 0.6, 0.7, 0.8, 0.9
Angle of Attack (deg)	-20, -19, -18, -17, -16, -15, -14, -13, -12, -11, -10, -9, -8, -7, -6, -5, -4, -3, -2, -1, 0, 1, 2, 3, 4, 5, 6, 7, 8, 9, 10, 11, 12, 13, 14, 15, 16, 17, 18, 19, 20

2.5 Creating the C81 Tables: Viterna-Corrigan Correction

Since the OVERFLOW simulations were only run for angles of attack of -20 to +20 degrees, they must be filled in beyond those points to account for rotor stall conditions. In order for the airfoil tables to be truly generalized, they should cover the full possible angle of attack range from -180º to +180º with reasonable data. NACA 0012 experimental data at the appropriate Reynolds number was used in this work as an approximation of airfoil performance beyond stall, where the airfoil performs, practically speaking, as a flat plate, Refs. [14-15]. The OVERFLOW simulation data was blended into the NACA 0012 data using the Viterna-Corrigan correction, which is an empirical approach for extrapolating post-stall sectional airfoil performance based on flat-plate theory and the rotor dimensions, Refs. [15-16]. Figure 5, reproduced from

Reference [17], shows a sample lift coefficient distribution over the full possible angle of attack range using the approach described above. Additional details can be found there.

The final C81 tables for the four HVAB airfoil coordinate files are provided in Appendix I.

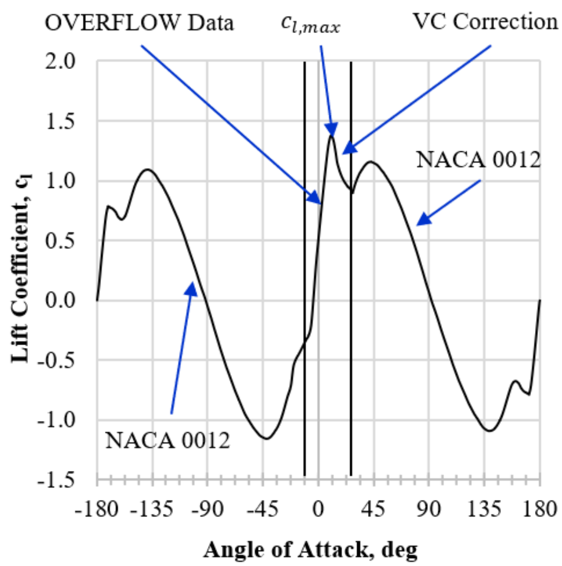

Figure 5. C81 Table Creation Using the Viterna-Corrigan Correction to Blend into NACA 0012 Data.

3 Summary

This work described the creation of C81 airfoil performance lookup tables generated in support of the NASA Hover Validation and Acoustic Baseline (HVAB) Test Campaign. C81 tables were generated for four airfoil profiles previously documented in the experimental test campaign preparation; they are the: RC4-12, RC4-10, RC6-08, and the RC6-08$_T$ airfoils. The AFTGen tool was used as a wrapper for the OVERFLOW CFD solver to simulate these airfoils over a wide range of Mach numbers and angles of attack relevant to rotorcraft problems. The simulated Reynolds numbers correspond to those of the HVAB rotor testing in the NASA Ames Research Center's National Full-Scale Aerodynamics Complex. Roughly 1,500 OVERFLOW simulations (2nd order accurate in time and 4th order accurate in space) were run using high point-density grids on the NASA High-End Computing Capability. These simulation data were then blended with NACA 0012 experimental data to create C81 tables covering the full possible angle of attack range from -180º to +180º. Although these C81 tables are tailored for HVAB rotor analyses using various predictive tools (e.g., comprehensive analysis, blade element theory, and hybrid CFD-BET methods), they are general and can be used as standalone airfoil performance lookup tables for the airfoils of interest.

Appendix I contains the airfoil coordinate files used in AFTGen (reproduced from Ref. [7]) and the fully turbulent C81 airfoil performance lookup tables created using the methods described in this work.

References

1) Norman, T. R, Heineck, J. T., Shairer, E. T., Schaeffler, N. W., Wagner, L. N., Yamauchi, G. K., Overmeyer, A. D., Ramasamy, M., Cameron, C. G., Dominguez, M., and Sheikman, A. L., "Fundamental Test of a Hovering Rotor: Comprehensive Measurements for CFD Validation," VFS Forum 79, West Palm Beach, FL, May 16-18, 2023. https://rotorcraft.arc.nasa.gov/Publications/files/79-2023-1166-Norman.pdf
2) *Hover Validation and Acoustic Baseline*, NASA Ames Research Center Aeromechanics Office, last updated February 2025. https://rotorcraft.arc.nasa.gov/HVAB/
3) Patt, D., and Youngren, H., "Improving Blade-Element Design Methods for High Speed Proprotors," AHS Specialists' Conference on Aeromechanics, San Francisco, CA, Jan. 2010. https://vtol.org/store/product/improving-bladeelement-design-methods-for-high-speed-proprotors-10658.cfm
4) Cornelius, J., and Schmitz, S., "Rotor Performance Predictions for UAM–Single vs Coaxial Rigid Rotors," VFS Transformative Vertical Flight Conference, San Jose, CA 2022. https://rotorcraft.arc.nasa.gov/Publications/files/Jason_Cornelius_Schmitz_12-Jan-22.pdf
5) OVERFLOW 2.3d, Overset Grid Computational Fluid Dynamics Flow Solver with Moving Body Capability (OVERFLOW), NASA Software Catalog, 2023. https://software.nasa.gov/software/LAR-20095-1
6) C81 Airfoil Table Generator using ARC2D (Efficient Two-Dimensional Solution Methods for The Navier-Stokes Equations), Sukra Helitek, Inc., Software Package, Build: July 2018, Ames, IA. http://sukra-helitek.com/
7) Overmeyer, A., Copp, P., Schaeffler, N., "Hover Validation and Acoustic Baseline Blade Set Definition," NASA/TM-2020-5002153. https://ntrs.nasa.gov/citations/20205002153
8) Noonan, K., U.S. Patent No. 4,412,664, Nov. 1, 1983.
9) Noonan, K., U.S. Patent No. 4,776,531, Oct. 11, 1988.
10) Noonan, K., "Aerodynamic Characteristics of Two Rotorcraft Airfoils Designed for Application to the Inboard Region of a Main Rotor Blade," NASA TM-3009, July 1990. https://ntrs.nasa.gov/citations/19900014923
11) Noonan, K., "Aerodynamic Characteristics of a Rotorcraft Airfoil Designed for the Tip Region of a Main Rotor Blade," NASA TM-4264, May 1993. https://ntrs.nasa.gov/citations/19930020261
12) Jain, R., "CFD Hover Performance and Transition Predictions on the PSP and HVAB Rotors Using CREATE-AV Helios," AIAA SciTech Forum, San Diego, CA, Jan. 3-7, 2022. https://doi.org/10.2514/6.2022-1549
13) AFTGen Airfoil Table Generator, Software Package, Build: 0.10.2, 2023. http://sukra-helitek.com/
14) Critzos, C., Heyson, H., and Boswinkle, R., "Aerodynamic Characteristics of NACA 0012 Airfoil Section at Angles of Attack From 0-180 Degrees," NACA TN-3361, Jan. 1955. https://ntrs.nasa.gov/citations/19930084501
15) Viterna, L., and Corrigan, R., "Fixed Pitch Rotor Performance of Large Horizontal Axis Wind Turbines," DOE/NASA Workshop on Large Horizontal Axis Wind Turbines, published online Jan. 1982. https://ntrs.nasa.gov/citations/19830010962
16) Tangler, J., and Kocurek, D., "Wind Turbine Post-Stall Airfoil Performance Characteristics Guidelines for Blade-Element Momentum Methods," 43rd AIAA Aerospace Sciences Meeting and Exhibit, AIAA-2005-591, Reno, NV, 2005. https://doi.org/10.2514/6.2005-591
17) Cornelius, J., "Mid-Fidelity Performance Analysis for Fixed-Pitch Speed-Controlled Multirotor Aircraft," Dissertation in Aerospace Engineering, The Pennsylvania State University, Aug. 2023. https://etda.libraries.psu.edu/catalog/20665joc5693

Appendix I: HVAB Airfoil Coordinate Files and C81 Tables

HVAB rotor airfoil coordinate files are reproduced here from Reference [7]. The below embedded C81 tables were developed using the methods described in this NASA TM. Here is a brief overview of the most pertinent highlights:

- OVERFLOW version 2.3d flow solver, released February 19th, 2021,
- Fully-turbulent Spalart-Allmaras turbulence closure,
- 2nd order accurate in time and fourth order accurate in space,
- NACA 0012 experimental data used outside of +/- 20 degrees angle of attack,
- Viterna-Corrigan correction used to blend between OVERFLOW simulation data and NACA 0012 experimental data (see Section 2.5 for more detail).

<u>HVAB rotor C81 airfoil performance tables:</u>

1. RC4-10
   a. High-density Airfoil Coordinate File:
   b. HVAB Rotor C81 Table:
2. RC4-12
   a. High-density Airfoil Coordinate File:
   b. HVAB Rotor C81 Table:
3. RC6-08
   a. High-density Airfoil Coordinate File:
   b. HVAB Rotor C81 Table:
4. RC6-08$_{T}$
   a. High-density Airfoil Coordinate File:
   b. HVAB Rotor C81 Table: